Structural Engineering and Mechanics, Vol. 22, No. 5 (2006) 575-597
DOI: http://dx.doi.org/10.12989/sem.2006.22.5.575

Enhanced finite element modeling for geometric non-linear analysis of cable-supported structures

Myung-Kwan Song†

Department of Specific Structures, Chungsuk Engineering Co., Ltd, Seoul 138-802, Korea

Sun-Hoon Kim‡

Department of Civil and Environmental Engineering, Youngdong University, Chungbuk 370-701, Korea

Chang-Koon Choi‡†

Department of Civil and Environmental Engineering, KAIST, Daejeon 305-701, Korea

(Received February 16, 2005, Accepted January 10, 2006)

Abstract. Enhanced three-dimensional finite elements for geometrically nonlinear analysis of cable-supported structures are presented. The cable element, derived by using the concept of an equivalent modulus of elasticity and assuming the deflection curve of a cable as catenary function, is proposed to model the cables. The stability functions for a frame member are modified to obtain a numerically stable solution. Various numerical examples are solved to illustrate the versatility and efficiency of the proposed finite element model. It is shown that the finite elements proposed in this study can be very useful for geometrically nonlinear analysis as well as free vibration analysis of three-dimensional cable-supported structures.

Keywords: cable-supported structures; geometric nonlinear analysis; free vibration analysis; cable element; frame element; stability function.

1. Introduction

Cable-supported structures are used extensively to support cable-stayed bridges, suspension bridges, offshore structures, long span roofs, communication towers, and so on. Such structures are often more economical than conventional ones because of the high efficiency of steel members in simple tension. However, cable-supported structures are quite flexible so that they may undergo large displacements before attaining their equilibrium configuration. Consequently, a more challenging geometric nonlinear analysis may well be required.

Analytical methods have been employed in the past mainly for quite simple cable structures

† Assistant Director, Ph.D., E-mail: mksong@cse.co.kr
‡ Associate Professor, Ph.D., Corresponding author, E-mail: kimsh@youngdong.ac.kr
‡† Institute Chair Professor

(Irvine 1992). Dean (1961), Davenport and Steels (1965), and Veletsos and Darbre (1983) have presented theoretical formulae for computing equivalent spring constants for uniformly loaded cables. For cable roof structures, analysis methods and several very illustrative design details were studied by Buchholdt (1985).

As cable structures are increased with popularity, more efficient and accurate methods were searched and various cable modeling techniques could be found. Gambhir (1977) developed a two-node curved finite element using cubic polynomial interpolation functions and used for the static and dynamic analysis of three-dimensional prestressed cablenets. Ozdemir (1979) developed another two-node curved finite elements using Lagrangian functions for the interpolation of element geometry. Recently, derivations of isoparametric cable elements, which includes the element curvature, were presented (Leonard 1988) and a four-node isoparametric cable element was used for modeling cables in cable stayed bridges (Ali and Abdel-Ghaffar 1995). Karoumi (1999) developed two-node catenary cable element using exact analytical expressions for the elastic catenary and Desai and Punde (2001) proposed a simple cable element with nine degrees of freedom to describe vibrations of an inclined cable by using a generalized finite element approach.

However, although a number of researchers had studied the analysis of the non-linear behavior of cable-supported structures, the applications were so complicated that general engineers could not apply those cable elements for modeling cables with ease. In particular, when modeling cable in cable-stayed bridges, the truss elements with an equivalent cable stiffness are often adopted, which is referred to as the equivalent modulus approach and has been used by several investigators (Fleming 1979, Fleming and Egeseli 1980, Nazmy and Abdel-Ghaffar 1990, Boonyapinyo and Yamada 1994, Adeli and Zhang 1995, Karoumi 1996, Gimsing 1997, Monaco and Fiore 2005, Wang *et al*. 1998). The equivalent secant modulus of elasticity, used to take account of the sag effect, which was derived by Ernst (1965), can be written as follows;

$$E_{\text{sec}}^{c} = \frac{E_e}{1 + \left(\dfrac{(wl\cos\alpha)^2 (T_i + T_f) E_e A}{24 T_i^2 T_f^2} \right)} \tag{1}$$

where E_e is the modulus of elasticity of a cable, A is the cross-sectional area of a cable, w is the self weight of a cable, l is the cable length, and α is the inclined angle of a cable.

This study places emphasis on the simple finite element modeling aspect of cable-stayed bridges. Cable and frame finite elements are derived for modeling cable-stayed structures. The equivalent modulus of elasticity as shown in Eq. (1), which is used in cable element, is enhanced. And, the stability, which is used in frame element, is modified for stable solutions. Various numerical examples are solved to illustrate the versatility and efficiency of the proposed model.

2. Finite element model of a cable

An equivalent modulus of elasticity for the cable having sag is frequently used in the cable-supported structures. Cables are only supported to resist axial tensile force. Thus, they have large deformations under the external forces and show the dramatically nonlinear structural behaviors. There are several useful methods to model the geometrical nonlinear behavior of cables, in which elastic catenary cable elements and truss elements with the equivalent modulus of elasticity are

included. The method to use the truss element with an equivalent modulus of elasticity derived by Ernst (1965) has solutions with some errors as sag becomes large, because the method assumes that deflection curve is a parabolic function. Some elastic catenary cable elements have so difficult formulations that general engineers cannot apply with ease. Therefore, in this study, the equivalent modulus of elasticity of a cable having sag, which is simple and enhanced, is derived by the use of catenary function.

2.1 Equivalent modulus of elasticity

Two cables in the different loading conditions are considered to derive the equations of the equivalent modulus of elasticity of a cable. In Fig. 1, tensile force T_i is being loaded to a cable and in Fig. 2, the tensile force T_i is increased to T_f.

The catenary cable function before the increase of the tensile force in Fig. 1 is as follows;

$$y = \frac{T_i}{w}\left\{\cosh\left[\frac{w}{T_i}\left(x-\frac{1}{2}L_c\right)\right]-\cosh\left(\frac{wL_c}{2T_i}\right)\right\} \tag{2}$$

where w is the self weight of a cable.

And, the catenary cable function after the increase of the tensile force in Fig. 2 is as follows;

$$y = \frac{T_f}{w}\left\{\cosh\left[\frac{w}{T_f}\left(x-\frac{L_c+\delta}{2}\right)\right]-\cosh\left(\frac{w(L_c+\delta)}{2T_f}\right)\right\} \tag{3}$$

Therefore, on the basis of the condition that the tensile force is zero, the total elongations of two cables under the tensile forces T_i and T_f are respectively as follow;

$$\Delta s_1 = \frac{T_i}{E_e A}\int_0^{L_c}\left[1+\left(\frac{dy}{dx}\right)^2\right]dx = \frac{T_i^2}{2E_e Aw}\left[\sinh\left(\frac{wL_c}{T_i}\right)+\frac{w}{T_i}\right] \tag{4}$$

$$\Delta s_2 = \frac{T_f^2}{2E_e Aw}\left[\sinh\left(\frac{wL_c}{T_f}\right)+\frac{wL_c}{T_f}\right] \tag{5}$$

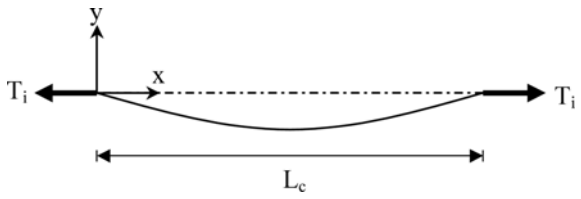

Fig. 1 Cable before the increase of tensile force

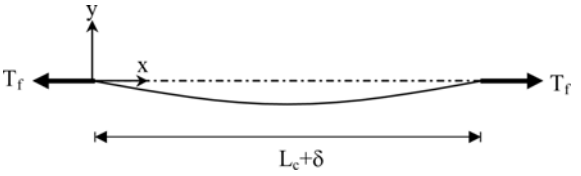

Fig. 2 Cable after the increase of tensile force

where E_e is the modulus of elasticity of a cable, A is the cross-sectional area of a cable, and it is assumed that δ is much smaller than L_c.

From Eqs. (4) and (5), the relative deformation of two cables $\delta(=\Delta s_1 - \Delta s_2)$ is derived as follows;

$$\delta = \frac{\frac{(T_f - T_i)L_c}{2E_eA} + \frac{1}{2E_eAw}\left[T_f^2 \sinh\left(\frac{wL_c}{T_f}\right) - T_i^2 \sinh\left(\frac{wL_c}{T_i}\right)\right]}{\cosh\left(\frac{wL_c}{2T_f}\right)} + \frac{\frac{2}{w}\left[T_i \sinh\left(\frac{wL_c}{2T_i}\right) - T_f \sinh\left(\frac{wL_c}{2T_f}\right)\right]}{\cosh\left(\frac{wL_c}{2T_f}\right)} \tag{6}$$

Thus, the secant modulus of elasticity of a cable can be derived by the use of Eq. (6) as follows;

$$E_{\text{sec}}^c = \frac{\frac{(T_f - T_i)}{A}}{\frac{\delta}{L_c}} \tag{7}$$

Therefore, finally, the equivalent secant modulus of elasticity E_{sec}^c of a cable with the angle of chord α in Fig. 3 can be derived as follows;

$$E_{\text{sec}}^c = \frac{E_e}{(1 + C_1 + C_2)/2\cosh\left(\frac{wL_c\cos\alpha}{2T_f}\right)} \tag{8}$$

where

$$C_1 = \frac{1}{wL_c\cos\alpha(T_f - T_i)}\left[T_f^2 \sinh\left(\frac{wL_c\cos\alpha}{T_f}\right) - T_i^2 \sinh\left(\frac{wL_c\cos\alpha}{T_i}\right)\right] \tag{9}$$

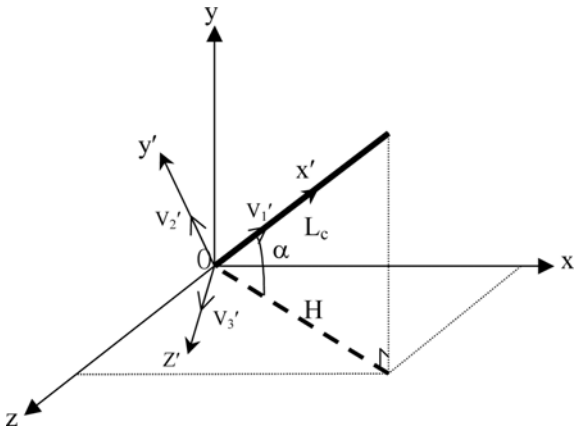

Fig. 3 Local axis and direction vector in cable element

$$C_2 = \frac{4E_eA}{wL_c\cos\alpha(T_f - T_i)}\left[T_i\sinh\left(\frac{wL_c\cos\alpha}{2T_i}\right) - T_f\sinh\left(\frac{wL_c\cos\alpha}{2T_f}\right)\right] \tag{10}$$

And, the equivalent tangent modulus of elasticity $E^c_{\tan}$ can be also expressed as follows;

$$E^c_{\tan} = \frac{E_e}{(1 + C_1 + C_2)/2\cosh\left(\frac{wL_c\cos\alpha}{2T}\right)} \tag{11}$$

where

$$C_1 = \frac{1}{wL_c\cos\alpha}\left[2T\sinh\left(\frac{wL_c\cos\alpha}{T}\right) - wL_c\cos\alpha\sinh\left(\frac{wL_c\cos\alpha}{T}\right)\right] \tag{12}$$

$$C_2 = \frac{-4E_eA}{wL_c\cos\alpha}\left[\sinh\left(\frac{wL_c\cos\alpha}{2T}\right) - \frac{wL_c\cos\alpha}{2T}\cosh\left(\frac{wL_c\cos\alpha}{2T}\right)\right] \tag{13}$$

The equivalent secant modulus of elasticity derived by Ernst (1965) in Eq. (1) can be derived by substituting only the first term of Eq. (6) for Eq. (7). In other words, the more nonlinear terms in Eqs. (8) and (11) than in Eq. (1) are used to take account of the influence of sag effect.

2.2 Element stiffness matrix

The degrees of freedom of a cable element are defined as shown in Fig. 4. The axial stiffness of the cable element can be expressed with the help of the equivalent modulus of elasticity E_{eq}. The element tangent stiffness matrix of a cable $[K_t]_c$ can be given by

$$[K_t]_c = [K_e]_c + [K_g]_c \tag{14}$$

where $[K_e]_c$ is the elastic stiffness matrix and $[K_g]_c$ is the geometric stiffness matrix of a cable element (Nazmy and Abdel-Ghaffer 1990) (Appendix A). Using the direction vector in Fig. 3, the element tangent stiffness matrix can be defined in the global axis.

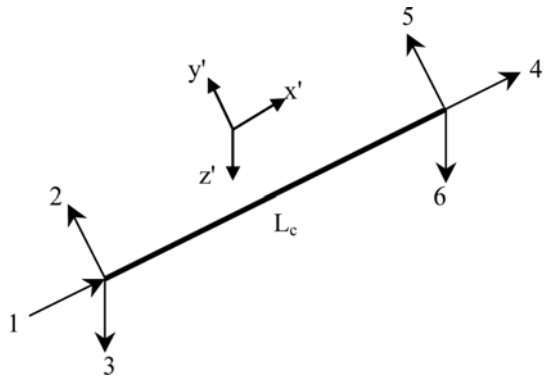

Fig. 4 Degrees of freedom in the local axis of cable element

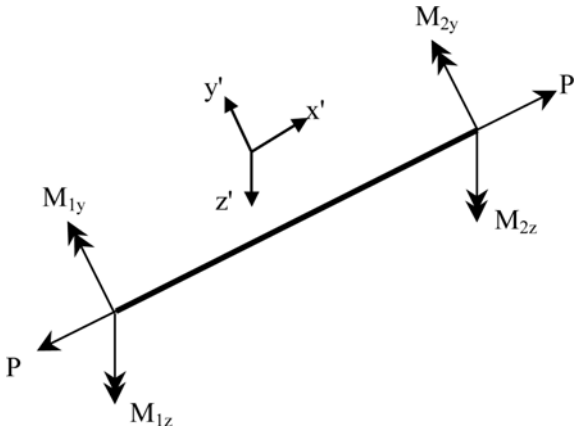

Fig. 5 Axial force and bending moment in frame element

3. Finite element model of a frame member

The large deformations that occur in the frame members of a cable-supported structures under the combined effect of large bending moments and high axial forces produce a strong coupling between axial and flexural stiffness in these members (Fig. 5). This coupling can be considered in the refined nonlinear analysis by introducing the concept of stability functions (Prezeminiecki 1969).

3.1 Element stiffness matrix

In this study, frame elements are adopted to model towers and girders in three-dimensional space. The degrees of freedom of a frame element are defined as shown in Fig. 6. The element tangent stiffness matrix of a frame $[K_t]_b$ can be given by

$$[K_t]_b = [K_e]_b + [K_g]_b \tag{15}$$

where $[K_e]_b$ is the elastic stiffness matrix of a frame element and $[K_g]_b$ is the geometric stiffness matrix of a frame element (See Appendix A). $[K_e]_b$, which is shown in Eq. (A.4) in the Appendix, is composed by using stability functions S_{1z}~S_{4z}, S_{1y}~S_{4y}, and S_5 (Fleming 1978).

When external loads are gradually increased, the principal moment of inertia axes in a frame member are changed by the influence of the torsional rotation (θ_{t1}) in a node. Thus, in each load incremental step, θ_{t1} should be modified to compose transformation matrix $[T]$ as shown in Eq. (16) (Tezcan 1969) (Fig. 7).

$$[T] = \begin{bmatrix} [t]_1 & 0 & 0 & 0 \\ & [t]_1 & 0 & 0 \\ & & [t]_2 & 0 \\ sym. & & & [t]_2 \end{bmatrix} \tag{16}$$

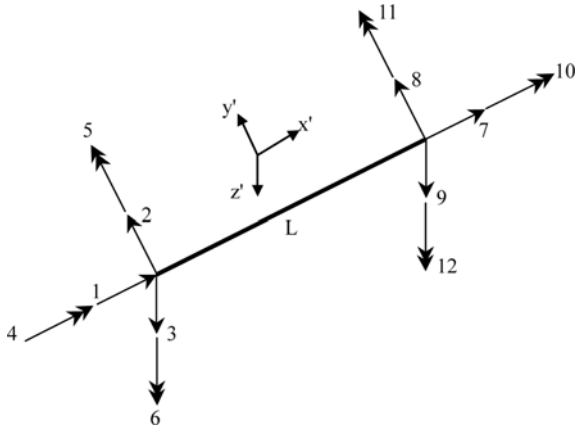

Fig. 6 Degrees of freedom in the local axis of frame element

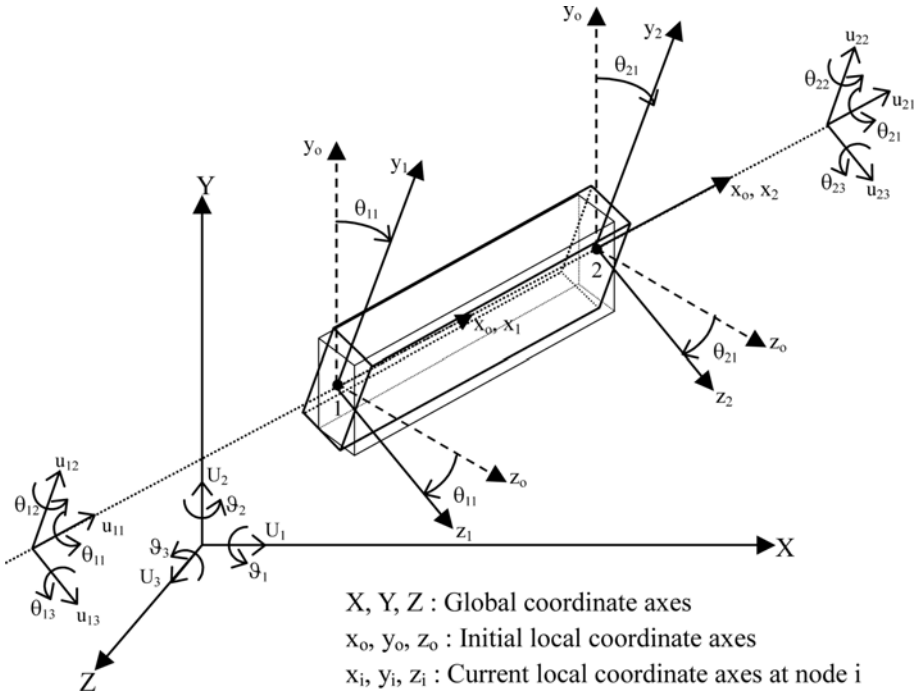

Fig. 7 Global axis and local axis of frame element

where

$$[t]_i = \begin{bmatrix} 1 & 0 & 0 \\ 0 & \cos\theta_{i1} & \sin\theta_{i1} \\ 0 & -\sin\theta_{i1} & \cos\theta_{i1} \end{bmatrix} \begin{bmatrix} l_{x'} & m_x & n_{x_0} \\ l_{y_0} & m_{y_0} & n_{y_0} \\ l_{z_0} & m_{z_0} & n_{z_0} \end{bmatrix} = [\beta]_i[\lambda]_0 \quad (i = 1, 2) \tag{17}$$

where $[\lambda]_0$ is initial directional vector, and $V_1' = \langle l_{x_0} \; m_{x_0} \; n_{x_0} \rangle$, $V_2' = \langle l_{y_0} \; m_{y_0} \; n_{y_0} \rangle$, and

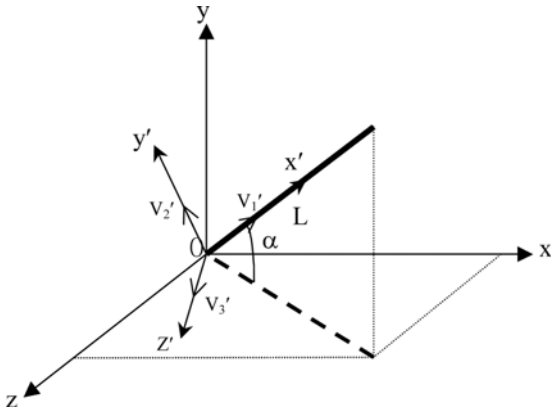

Fig. 8 Initial direction vector of frame element

$V_3' = \langle l_{z_0} \; m_{z_0} \; n_{z_0} \rangle$ are respective directional vectors of the initial local axes in a frame element (Fig. 8).

By the use of the modified transformation matrix $[T]$, the global stiffness matrix $[K_t]_b^G$ of a frame member can be made as follows;

$$[K_t]_b^G = [T]^T [K_t]_b [T] \tag{18}$$

For a cable member, it is needless to consider the influence of a torsional rotation in a node and the global stiffness matrix can be made by the use of the general transformation matrix.

3.2 Modification of stability functions

When the conventional stability functions given by Fleming (1978) are used without any modification, they occasionally give unstable solutions (Fig. 9). In order to remove this problem, they are modified thorough using Taylor's series expansion (Choi and Lee 1996).

In the case of tensile force P (P is positive),

$$S_{1z} = \left(1 + \frac{\omega_z^2}{6} + \frac{\omega_z^4}{120} + \frac{\omega_z^6}{5040} + \frac{\omega_z^8}{362880}\right)/R_t \tag{19}$$

$$S_{2z} = \left(1 + \frac{\omega_z^2}{12} + \frac{\omega_z^4}{360} + \frac{\omega_z^6}{20160} + \frac{\omega_z^8}{1814400}\right)/R_t \tag{20}$$

$$S_{3z} = \left(1 + \frac{\omega_z^2}{10} + \frac{\omega_z^4}{280} + \frac{\omega_z^6}{15120} + \frac{\omega_z^8}{1330560}\right)/R_t \tag{21}$$

$$S_{4z} = \left(1 + \frac{\omega_z^2}{20} + \frac{\omega_z^4}{840} + \frac{\omega_z^6}{60480} + \frac{\omega_z^8}{6652800}\right)/R_t \tag{22}$$

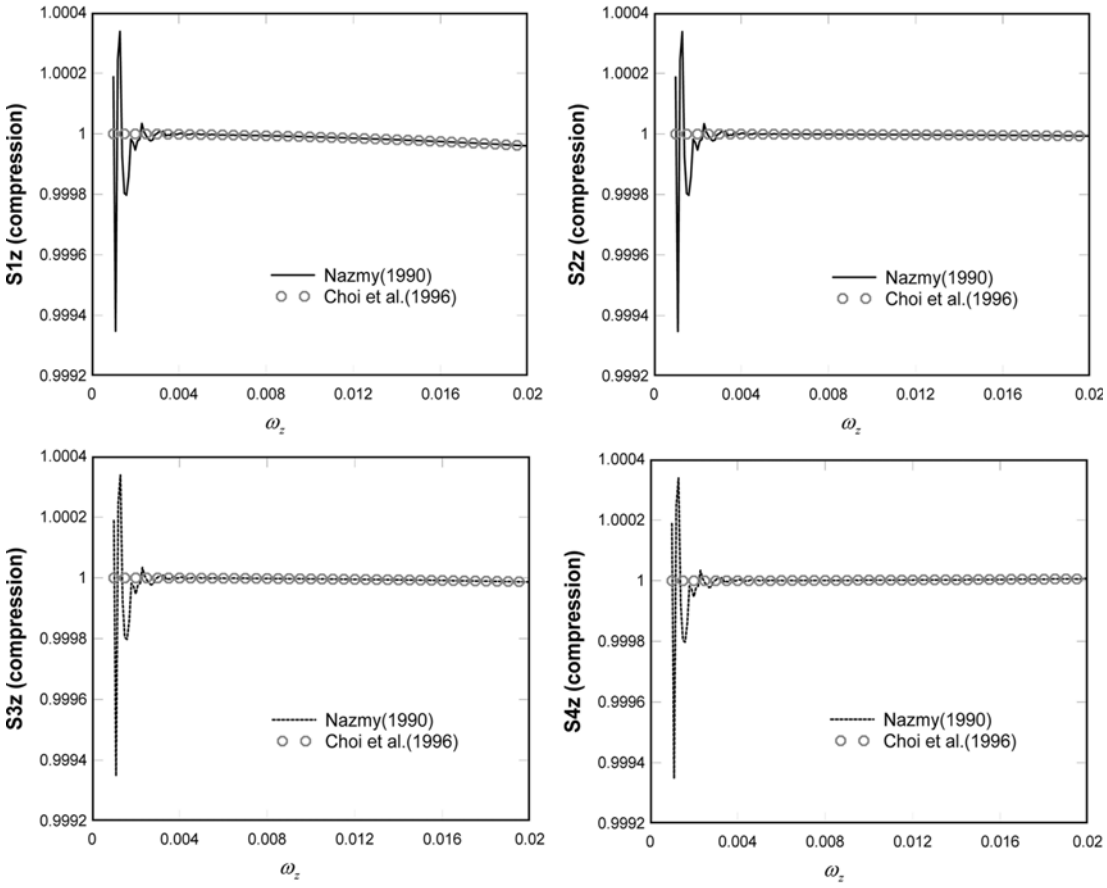

Fig. 9 Modification of stability functions

$$R_t = 1 + \frac{\omega_z^2}{15} + \frac{\omega_z^4}{560} + \frac{\omega_z^6}{37800} + \frac{\omega_z^8}{3991680} \tag{23}$$

where $\omega_z = \mu_z L$, $\mu_z^2 = \dfrac{P}{EI_z}$.

In the case of compressive force P (P is negative),

$$S_{1z} = \left(1 - \frac{\omega_z^2}{6} + \frac{\omega_z^4}{120} - \frac{\omega_z^6}{5040} + \frac{\omega_z^8}{362880}\right)/R_c \tag{24}$$

$$S_{2z} = \left(1 - \frac{\omega_z^2}{12} + \frac{\omega_z^4}{360} - \frac{\omega_z^6}{20160} + \frac{\omega_z^8}{1814400}\right)/R_c \tag{25}$$

$$S_{3z} = \left(1 - \frac{\omega_z^2}{10} + \frac{\omega_z^4}{280} - \frac{\omega_z^6}{15120} + \frac{\omega_z^8}{1330560}\right)/R_c \tag{26}$$

$$S_{4z} = \left(1 - \frac{\omega_z^2}{20} + \frac{\omega_z^4}{840} - \frac{\omega_z^6}{60480} + \frac{\omega_z^8}{6652800}\right)/R_c \tag{27}$$

$$R_c = 1 - \frac{\omega_z^2}{15} + \frac{\omega_z^4}{560} - \frac{\omega_z^6}{37800} + \frac{\omega_z^8}{3991680} \tag{28}$$

S_{1y}~S_{4y} are modified by the same way and S_5 is used as the same one with the conventional function (Appendix C).

3.3 Element mass matrix

A frame element with the degrees of freedom shown in Fig. 6 has the element mass matrix given in Eq. (B.1) in the Appendix (Przemieniecki 1968). In composing the element mass matrix of a cable element, it is assumed that $I_x = I_y = I_z = 0$ in Appendix (B.1).

4. Numerical analysis methods

4.1 Nonlinear static analysis

When structural analysis is performed by considering material nonlinearity and geometrical nonlinearity, structural responses are generally solved through iterative analysis because nonlinear terms are included in the stiffness matrix of the structure. In this paper, a combination of the incremental and iterative schemes is utilized. The load is applied incrementally, and iterations are performed after all the load increments (Nazmy and Abdel-Ghaffar 1990).

4.2 Free vibration analysis

In the first place, the nonlinear static analysis for the whole structure under the dead weight is performed and in this deformed structural shape, the stiffness matrix and mass matrix of the whole structure are composed. And then, by using these system matrices, free vibration analysis is fulfilled. In this paper, subspace iteration method is used to solve the eigenvalue problem. It is very useful to solve the main low-order free vibration mode (Cook *et al*. 1989).

5. Numerical examples

5.1 Cable under its own weight subjected to tensile force at both ends (sag ratio=1/10)

A cable hanging under its own weight and subjected to a tensile force along its chord, as shown in Fig. 10 was studied to verify the cable element. Using the different models, the sag and the longitudinal displacement along the chord of the cable were determined for different values of the tensile force T and the results are plotted in Fig. 11. Good agreement is observed when comparing the curves for the proposed cable element with those of other cable elements.

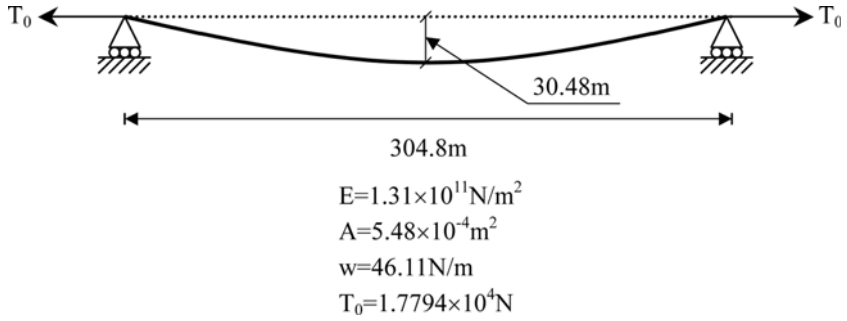

Fig. 10 Cable under its own weight and tensile force (sag ratio=1/10)

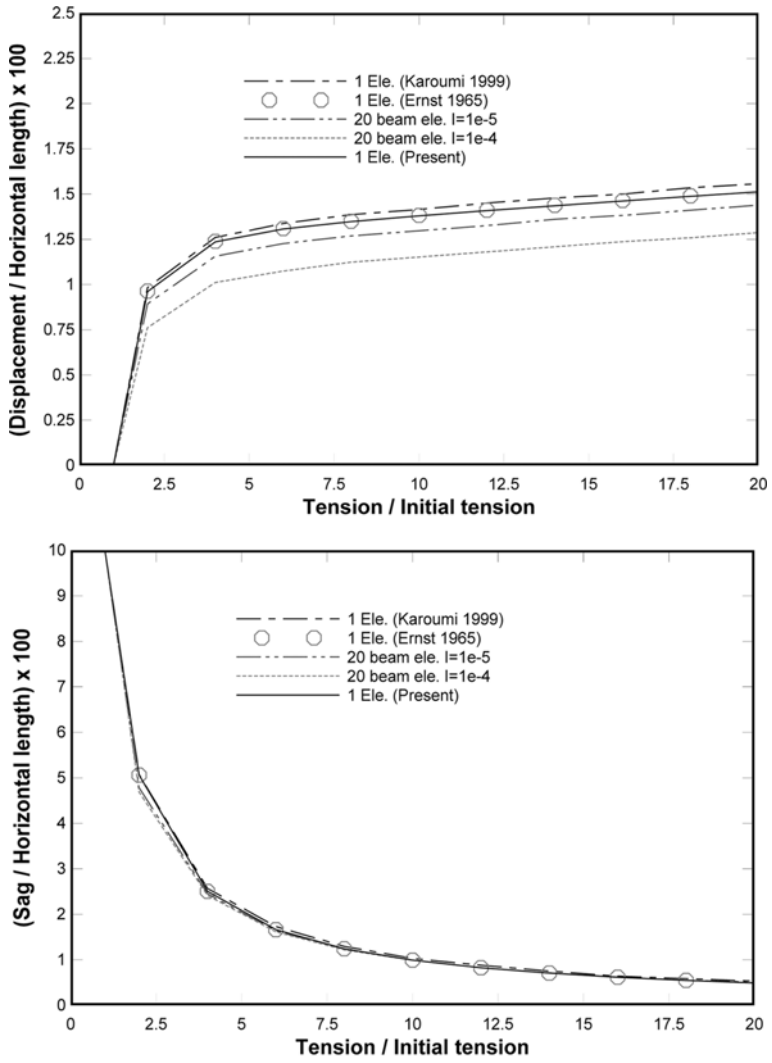

Fig. 11 Load-displacement relationship (sag ratio=1/10)

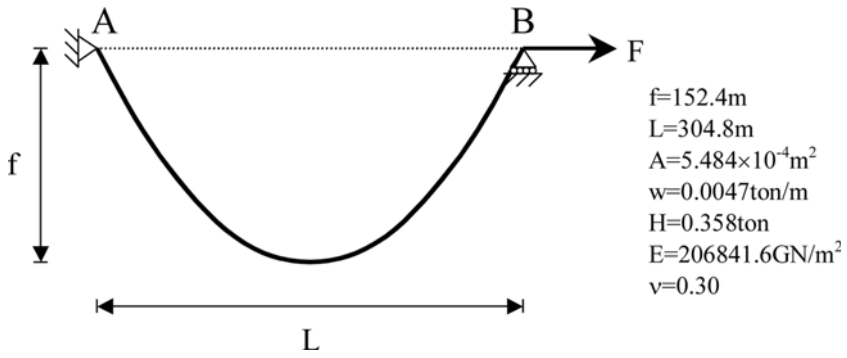

Fig. 12 Cable under its own weight and tensile force (sag ratio=1/2)

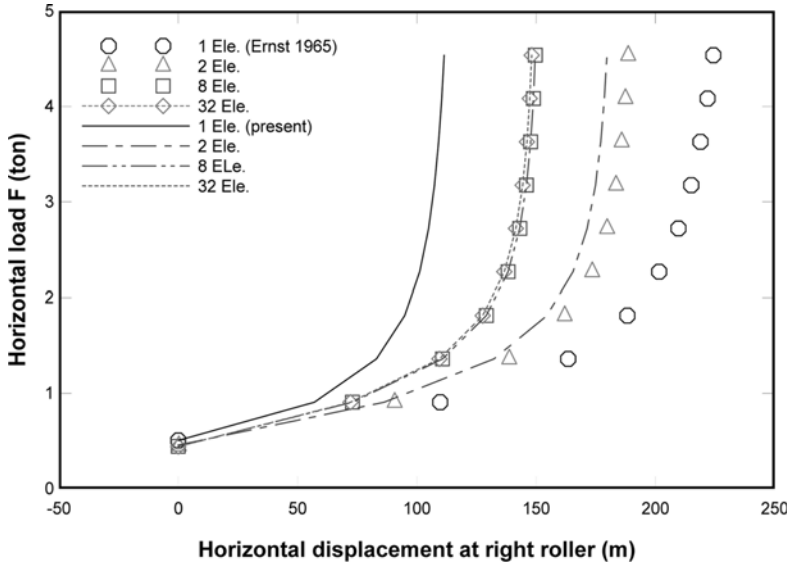

Fig. 13 Load-displacement relationship (sag ratio=1/2)

5.2 Cable under its own weight subjected to tensile force at both ends (sag ratio=1/2)

A cable hanging under its own weight and subjected to a tensile force along its chord, as shown in Fig. 12 is the second verification example of the proposed cable element. H(=0.358 ton) is the horizontal force to sustain the sag of 152.4 m under the self-weight of cable in the initial state. The analysis results using the proposed equivalent modulus of elasticity of a cable are compared with those using the equivalent modulus of elasticity of a cable proposed by Ernst (1965). As shown in Fig. 13 and Table 1, the horizontal displacement is converged to the constant value as the number of cable elements is increased. In the case that the number of cable elements is two, the differences between the two analysis results are clearly distinct. As the number of cable elements increase, the difference disappears.

Table 1 Comparisons of the horizontal displacements (Unit: m)

Cable tensile force (kg_f)			9,072	1,361	1,814	2,268	2,722	3,175	3,629	4,082	4,536
Numbers of elements	1	Ernst	109.730	163.410	188.240	201.560	209.640	215.020	218.900	221.870	224.270
		Present	57.018	83.030	94.887	101.180	104.940	107.400	109.120	110.410	111.410
		Error (%)	92.4	96.8	98.3	99.2	99.8	100.2	100.6	100.9	101.3
	2	Ernst	90.711	138.750	161.970	173.520	179.780	183.490	185.860	187.460	188.610
		Present	86.264	132.330	154.480	165.450	171.380	174.880	177.100	178.600	179.660
		Error (%)	5.2	4.9	4.9	4.9	4.9	4.9	4.9	5.0	5.0
	8	Ernst	73.002	110.770	129.130	138.250	143.130	145.960	147.720	148.870	149.660
		Present	72.981	110.740	129.110	138.220	143.100	145.930	147.690	148.840	149.630
		Error (%)	0.03	0.02	0.02	0.02	0.02	0.02	0.02	0.02	0.02
	32	Ernst	72.182	109.470	127.620	136.660	141.530	144.360	146.130	147.310	148.140
		Present	72.182	109.470	127.620	136.660	141.530	144.360	146.130	147.310	148.140
		Error (%)	0.	0.	0.	0.	0.	0.	0.	0.	0.

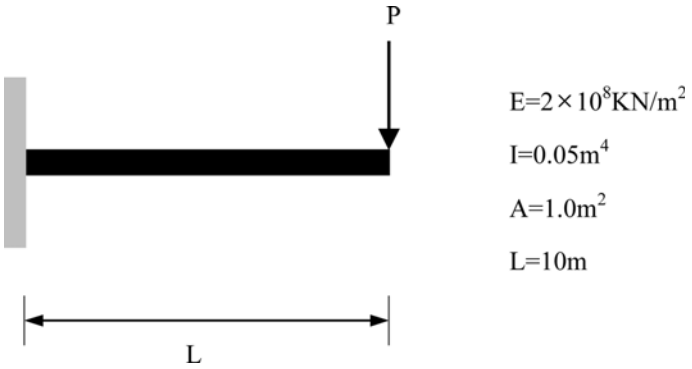

Fig. 14 Cantilever beam under vertical load

5.3 Cantilever beam under vertical load

For the verification of the formulation of a frame element, a cantilever beam under vertical load as shown in Fig. 14 is analyzed and the analysis results are compared with theoretical solutions (Hyundai 1994). The cantilever beam is modeled with 10 elements and the vertical displacements (δ_v), horizontal displacements (δ_h), and rotations (θ) at the right end are compared. Through comparing analysis results, good agreements are shown in Table 2.

5.4 Guyed tower subjected to a head load

The response of the rigidly encasted guyed mast illustrated in Fig. 15 was investigated for a head load of 222.3 kN applied at the tip of the mast in 10 equal increments. Horizontal tip displacement of the mast are compared with those obtained by other researchers for each load increment as shown in Fig. 16. It can be observed that there is a close agreement.

Table 2 Comparisons of the analysis results with the theoretical solutions

PL^2/EI	δ_v/L		δ_h/L		$\theta/2\pi$	
	Theoretical	Present	Theoretical	Present	Theoretical	Present
0.	0.	0.	0.	0.	0.	0.
0.2	0.066	0.066	0.003	0.003	0.063	0.063
0.4	0.131	0.131	0.010	0.010	0.126	0.126
0.6	0.192	0.192	0.022	0.022	0.185	0.185
0.8	0.249	0.250	0.038	0.038	0.241	0.241
1.	0.302	0.302	0.056	0.056	0.294	0.294
1.5	0.411	0.411	0.108	0.108	0.407	0.407
2.	0.493	0.494	0.161	0.160	0.498	0.498
3.	0.603	0.604	0.254	0.254	0.628	0.628
4.	0.670	0.672	0.329	0.328	0.714	0.715
5.	0.714	0.716	0.388	0.387	0.774	0.775
6.	0.745	0.747	0.435	0.434	0.817	0.818
7.	0.767	0.770	0.473	0.472	0.850	0.851
8.	0.785	0.788	0.505	0.504	0.875	0.876
9.	0.799	0.803	0.532	0.531	0.895	0.896
10.	0.811	0.815	0.555	0.554	0.911	0.912
15.	0.848	0.854	0.635	0.634	0.956	0.957

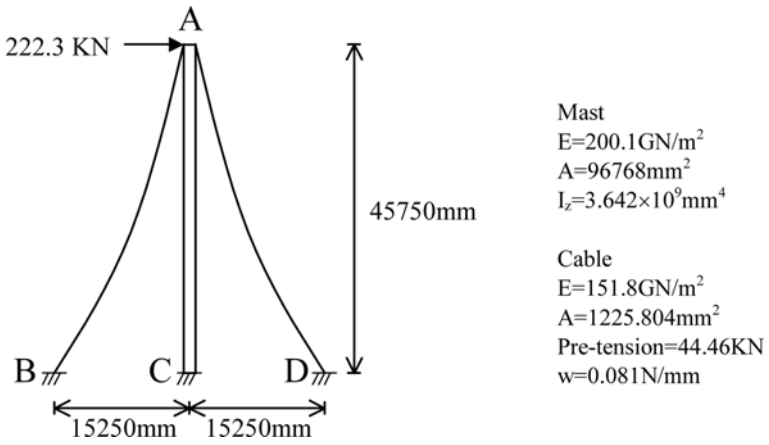

Fig. 15 Guyed tower subjected to a head load

5.5 Cantilever beam supported by an inclined cable

A cantilever beam supported by an inclined cable is modeled with 10 frame elements and 1 cable element as shown in Fig. 17. In this example, the analysis results are compared with those of elastic catenary cable elements (Hyundai 1994). The vertical deflections at node 7, in which the vertical deflection is largest, are compared with the other result. In spite of simple formulation, the analysis result in this study shows good agreement as shown in Table 3.

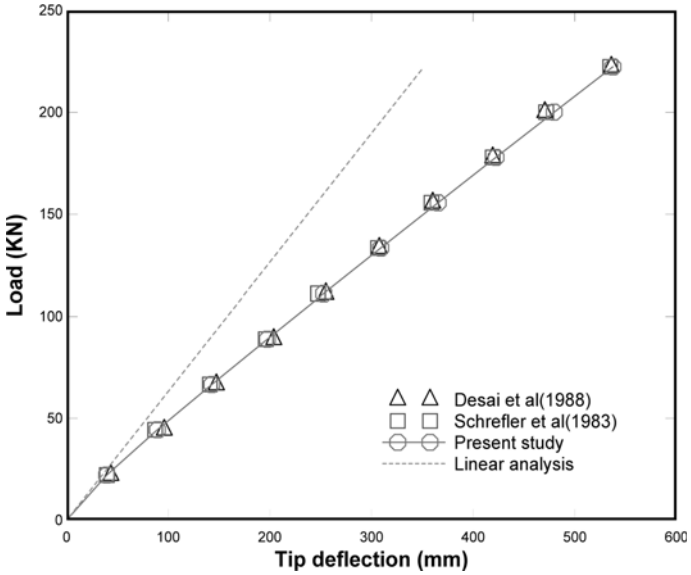

Fig. 16 Horizontal tip displacement on the head

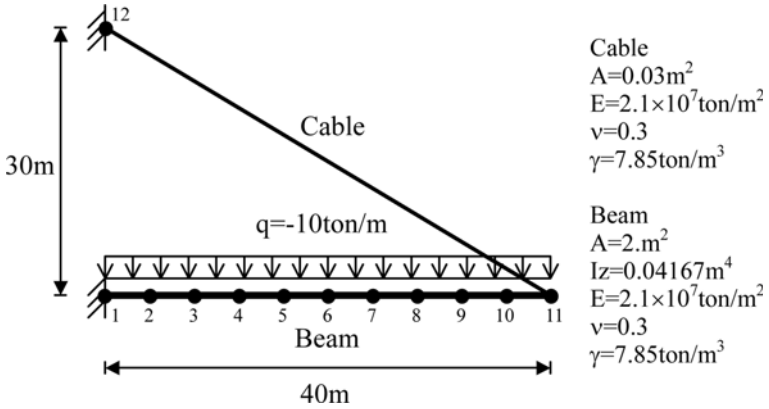

Fig. 17 Cantilever beam supported by inclined cable

Table 3 Comparisons of the vertical deflection at node 7 (Unit: m)

Cable tensile force (tonf)	Catenary cable element (Hyundai 1994)	Present
110.4	−0.47239	−0.47129
147.2	−0.46532	−0.46330
184.0	−0.46101	−0.45777
220.8	−0.45776	−0.45417

5.6 Two-dimensional cable-stayed bridge

A 2-D model of the cable-stayed bridge described in Karoumi (1999) was adopted for the

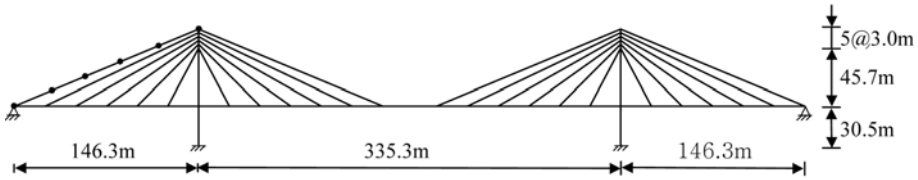

Fig. 18 Two-dimensional cable-stayed bridge

(a) Mode 1: $f_1 = 0.3264$ Hz (0.334 Hz)

(b) Mode 2: $f_2 = 0.4632$ Hz (0.437 Hz)

(c) Mode 3: $f_3 = 0.6918$ Hz (0.702 Hz)

*** Values inside a round bracket are reported in Karoumi (1999).**

Fig. 19 Natural frequencies and mode shapes for the lowest three vertical bending modes

verification for cable-stayed bridges. The geometry is depicted in Fig. 18, in which 120 cable elements to model cables and 44 frame elements are used to model stiffening girders and pylons. Results of free vibration frequencies analysis for this model were compared with those of Karoumi (1999), which are inserted in parentheses. As shown in Fig. 19, good agreement is obtained. Among the vertical bending modes, there are some free vibration modes, which result from the vibration of cables. For searching these modes, the free vibration analysis should be done through the refine division of cable elements, as in Karoumi (1998).

5.7 Three-dimensional cable-stayed bridge

The nonlinear static analysis and free vibration analysis of a 3-D cable-stayed bridge was adopted for final verification (Abdel-Ghaffar and Nazmy 1987, Nazmy and Abdel-Ghaffar 1990). The

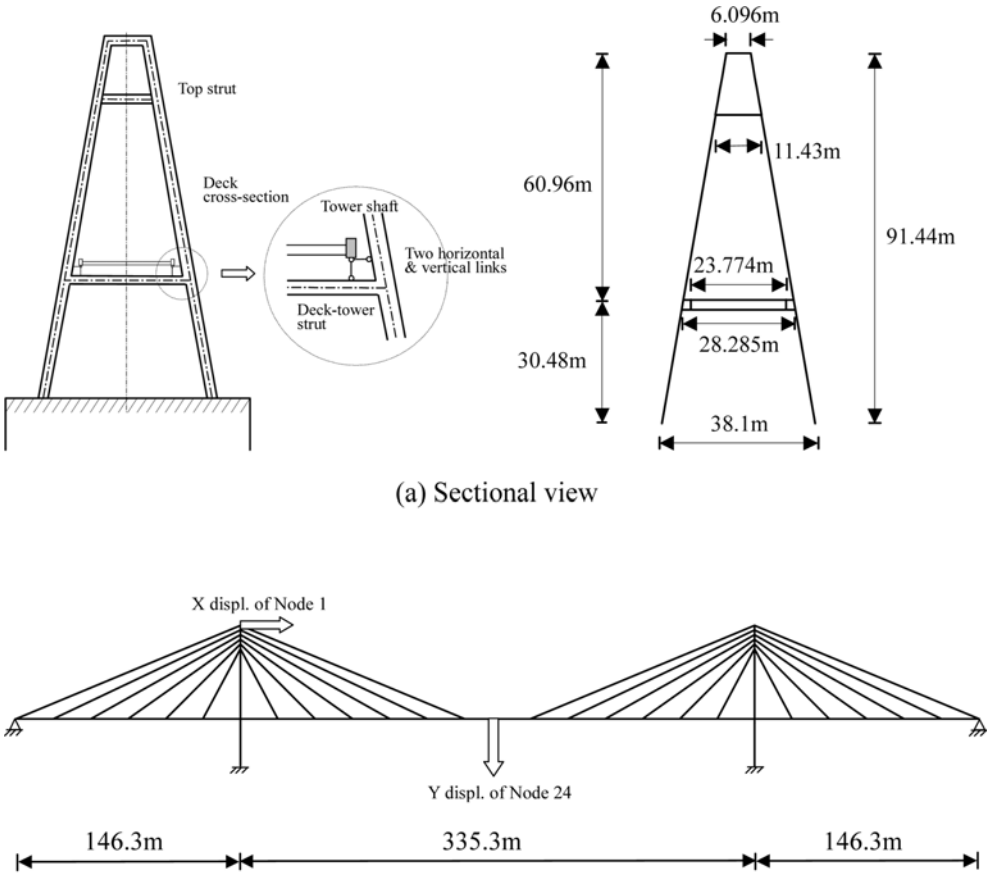

Fig. 20 Three-dimensional cable-stayed bridge

geometry is shown in Fig. 20, in which 48 cable elements for cables, 52 frame elements for stiffening girders, 42 frame elements for pylons, 27 frame elements for floor beams, and 8 frame elements for the connection between deck and pylons, are used.

The geometric nonlinear behavior of the cable-stayed bridge under initial cable tensile force and dead load are investigated at the points indicated in Fig. 20(b). When comparing the analysis results with those of Nazmy and Abdel-Ghaffar (1990), the improved cable elements and the modification of stability functions suggested in this paper show reasonable solutions although they make the difference of 4 percents (See Fig. 21).

Free vibration frequencies of this study were compared with those of Abdel-Ghaffar and Nazmy (1987) and good agreements were shown in Fig. 22. It is shown that torsional vibration mode can be not displayed in 2-D model but displayed in 3-D model. Therefore, it can be expected that the more accurate analysis results can be obtained by using the 3-D model.

In Fig. 23, the free vibration periods for three analysis models, which are classified by the supporting types on an abutment, are compared. The three supporting types studied in this study are

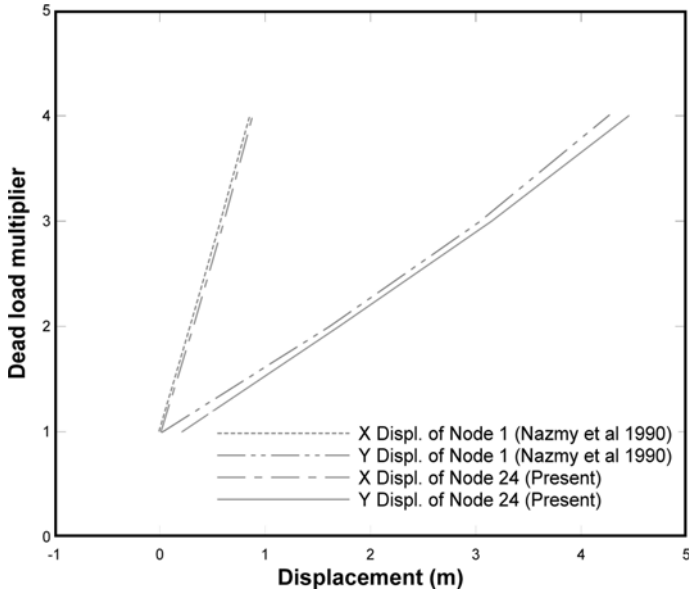

Fig. 21 Comparisons of the analysis results

(a) Mode 1: $f_1 = 0.3165$ Hz (0.3109 Hz), $T_1 = 3.1594$ sec

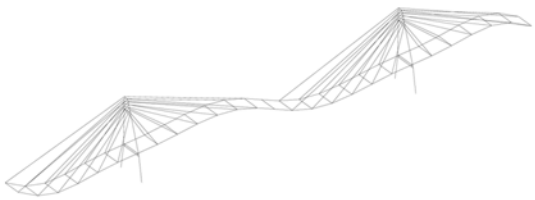

(b) Mode 2: $f_2 = 0.4583$ Hz (0.4105 Hz), $T_2 = 2.1878$ sec

(c) Mode 3: $f_3 = 0.5243$ Hz (0.5154 Hz), $T_3 = 1.9072$ sec

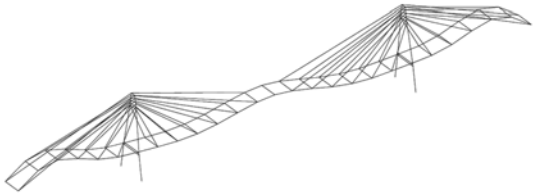

(d) Mode 4: $f_4 = 0.6691$ Hz (0.6498 Hz), $T_4 = 1.4946$ sec

*** Values inside a round bracket are reported in Karoumi (1999).**

Fig. 22 Natural vibration frequencies and mode shapes

hinge-hinge, hinge-roller, and roller-roller supporting conditions. As can be noticed, the differences of free vibration periods according to supporting types are larger for the lower-order modes than for the higher order modes. For the model of the hinge-hinge supporting type, the free vibration periods are shortest and for the roller-roller supporting type, those are longest. For example, the difference between two types is almost 17 percents for the second mode.

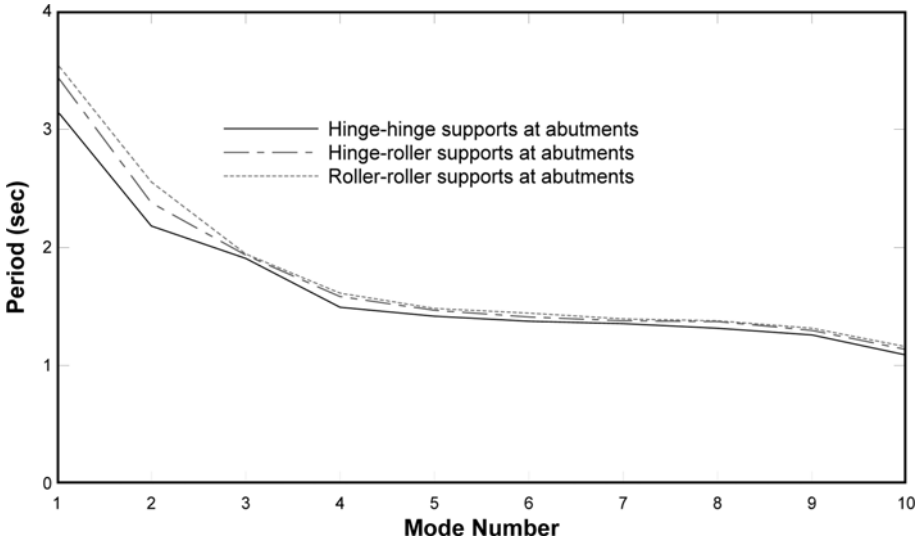

Fig. 23 Natural vibration periods of three analysis models according to abutment supporting types

6. Conclusions

Enhanced and efficient 3-dimensional finite elements for the structural analysis of cable-stayed bridges are presented in this study. The cable element for the modeling of cables is derived by using the concept of an equivalent modulus of elasticity and by assuming the catenary function as deflection curve of a cable. The frame element for modeling the bridge deck and the pylons is modified through using Taylor's series expansion as the stability functions to obtain a numerically stable solution. Various benchmark problems, in which comparable solutions exist, were performed to verify the accuracy and efficiency of the proposed finite elements. The numerical examples have illustrated that the proposed finite elements could be very useful for geometrically nonlinear analysis as well as free vibration analysis of 3-dimensional cable-stayed bridges through analyzing numerical examples.

Acknowledgements

The research work has been partially supported by the SISTEC (Smart Infra-Structure Technology Center) and Youngdong University. This support is greatly appreciated.

References

Abdel-Ghaffar, M. and Nazmy, A.S. (1987), "Effect of three-dimensionality and nonlinearity on the dynamic and seismic behavior of cable-stayed bridges", *Proc. of the 4th Structures Congress 1987 Vol. on Bridges and Transmission Line Structures*, ASCE, Orlando, August, 389-404.

Adeli, H. and Zhang, J. (1995), "Fully nonlinear analysis of composite girder cable-stayed bridges", *Comput.*

Struct., **54**, 267-277.
Ali, H.M. and Abdel-Ghaffar, A.M. (1995), "Modeling the nonlinear seismic behavior of cable stayed bridges with passive control bearings", *Comput. Struct.*, **54**, 461-492.
Boonyapinyo, V. and Yamada, H. (1994), "Wind-induced nonlinear lateral-torsional buckling of cable-stayed bridges", *J. Struct. Eng.,* ASCE, **120**, 486-506.
Bruno, D. and Grimaldi, A. (1985), "Nonlinear behavior of long-span cable-stayed bridges", *Meccanica*, **20**, 303-313.
Buchholdt, H.A. (1985), *An Introduction to Cable Roof Structures*, Cambridge: Cambridge University Press.
Choi, C.K., Lee, T.Y., Hong, H.S. and Kim, E.S. (1996), "A study on the evolutionary optimization of cable area of the cable-stayed bridge", *Proc. of the Computational Structural Engineering Institute Conference - October*, 113-120.
Cook, R.D., Malkus, D.S. and Plesha, M.Z. (1989), *Concepts and Applications of Finite Element Analysis*, 3rd Edition, John Wiley & Sons., USA.
Davenport, A.G. and Steels, G.N. (1965), "Dynamic behavior of massive guy cables", *J. Struct. Div.,* ASCE, **91**(2), 43-70.
Dean, D.L. (1961), "Static and dynamic analysis of guy cables", *J. Struct. Div.*, ASCE, **87**(1), 87-98.
Desai, Y.M. and Punde, S. (2001), "Simple mode for dynamic analysis of cable supported structures", *Eng. Struct.*, **23**, 271-279.
Desai, Y.M., Popplewell, N., Shan, A.H. and Buragohain, D.N. (1988), "Geometric nonlinear static analysis of cable supported structures", *Comput. Struct.*, **29**(6), 1001-1009.
Fleming, J.F. (1979), "Nonlinear static analysis of cable-stayed structures", *Comput. Struct.*, **10**, 621-635.
Fleming, J.F. and Egeseli, E.A. (1980), "Dynamic behavior of a cable-stayed bridge", *Earthq. Eng. Struct. Dyn.*, **8**, 1-16.
Gambhir, M.L. and Batchelor, B. (1977), "A finite element for 3-D prestressed cablenets", *Int. J. Numer. Meth. Eng.,* **11**, 1699-1718.
Gimsing, N.J. (1997), *Cable Supported Bridges*, 2nd Ed., Chichester: John Wiley.
Hyundai Institute of Construction Technology (1994), "Development of structural analysis system for the construction stage of cable suspension bridges", Final Reports, 1994.
Irvine, H.M. (1992), *Cable Structures*, New York: Dover Publications, Inc.
Karoumi, R. (1996), "Dynamic response of cable-stayed bridges subjected to moving vehicles", In: *IABSE 15th Congress*, Denmark, 87-92.
Karoumi, R. (1998), "Response at cable-stayed and suspension bridges to moving vehicles – analysis methods and practical modeling techniques", Doctoral Thesis, TRITA-BKN Bulletin 44, The Royal Institute at Technology, Stockholm, Sweden.
Karoumi, R. (1999), "Some modeling aspects in the nonlinear finite element analysis of cable supported bridges", *Comput. Struct.*, **71**, 397-412.
Leonard, J.W. (1988), *Tension Structures*, New York: McGraw-Hill.
Monaco, P. and Fiore, A. (2005), "A method to evaluate the frequencies of free transversal vibrations in self-anchored cable-stayed bridge", *Computers and Concrete*, **2**(2), 125-146.
Nazmy, A.S. and Abdel-Ghaffar, M. (1990), "Three-dimensional nonlinear static analysis of cable-stayed bridges", *Comput. Struct.*, **34**(2), 257-271.
Ozdemir, H. (1979), "A finite element approach for cable problems", *Int. J. Solids Struct.*, **15**, 427-437.
Prezeminiecki, J.S. (1969), *Theory of Matrix Structural Analysis*, McGraw-Hill Company, USA.
Schrefler, B.A., Odorezzi, S. and Wood, R.D. (1983), "A total Lagrangian geometrically nonlinear analysis of combined beam and cable structures", *Comput. Struct.*, **17**(1), 115-127.
Tezcan, S.S. and Mahapatra, B.C. (1969), "Tangent stiffness matrix for space frame members", *J. Struct. Div.*, ASCE, ST6, **95**, 1257-1270.
Veletsos, A.S. and Darbre, G.R. (1983), "Dynamic stiffness of parabolic cables", *Int. J. Earthq. Eng. Struct. Dyn.*, **11**(3), 367-401.
Wang, P.H., Lee, M.J. and Juang, H.J. (1998), "Study on cable equivalent modulus of elasticity", *Proc. the Sixth East Asia-Pacific Conf. on Structural Engineering and Construction*, Taiwan, January, 459-464.

Appendix

A. Element stiffness matrix

$$[K_e]_c = \frac{AE_{eq}}{L_c}\begin{bmatrix} 1 & 0 & 0 & -1 & 0 & 0 \\ & 0 & 0 & 0 & 0 & 0 \\ & & 0 & 0 & 0 & 0 \\ & & & 1 & 0 & 0 \\ & sym. & & & 0 & 0 \\ & & & & & 0 \end{bmatrix} \tag{A.1}$$

where $E_{eq} = E^c_{\sec}$ (or $E^c_{\tan}$).

$$[K_g]_c = \begin{bmatrix} [G]_c & -[G]_c \\ sym. & [G]_c \end{bmatrix}_{6\times 6} \tag{A.2}$$

where

$$[G]_c = \frac{T}{L_c}\begin{bmatrix} 0 & 0 & 0 \\ & 1 & 0 \\ sym. & & 1 \end{bmatrix} \tag{A.3}$$

where T is the tensile force of a cable.

$$[K_e]_b = \begin{bmatrix} \frac{EA}{L}S_5 & 0 & 0 & 0 & 0 & 0 & -\frac{EA}{L}S_5 & 0 & 0 & 0 & 0 & 0 \\ & \frac{12EI_z}{L^3}S_{1z} & 0 & 0 & 0 & \frac{6EI_z}{L^2}S_{2z} & 0 & -\frac{12EI_z}{L^3}S_{1z} & 0 & 0 & 0 & \frac{6EI_z}{L^2}S_{2z} \\ & & \frac{12EI_y}{L^3}S_{1y} & 0 & -\frac{6EI_y}{L^2}S_{2y} & 0 & 0 & 0 & -\frac{12EI_y}{L^3}S_{1y} & 0 & -\frac{6EI_y}{L^2}S_{2y} & 0 \\ & & & \frac{GJ}{L} & 0 & 0 & 0 & 0 & 0 & -\frac{GJ}{L} & 0 & 0 \\ & & & & \frac{4EI_y}{L}S_{3y} & 0 & 0 & 0 & \frac{6EI_y}{L^2}S_{2y} & 0 & \frac{2EI_y}{L}S_{4y} & 0 \\ & & & & & \frac{4EI_z}{L}S_{3z} & 0 & -\frac{6EI_z}{L^2}S_{2z} & 0 & 0 & 0 & \frac{2EI_z}{L}S_{4z} \\ & & & & & & \frac{EA}{L}S_5 & 0 & 0 & 0 & 0 & 0 \\ & & & & & & & \frac{12EI_z}{L^3}S_{1z} & 0 & 0 & 0 & -\frac{6EI_z}{L^2}S_{2z} \\ & & & sym. & & & & & \frac{12EI_y}{L^3}S_{1y} & 0 & \frac{6EI_y}{L^2}S_{2y} & 0 \\ & & & & & & & & & \frac{GJ}{L} & 0 & 0 \\ & & & & & & & & & & \frac{4EI_y}{L}S_{3y} & 0 \\ & & & & & & & & & & & \frac{4EI_z}{L}S_{3z} \end{bmatrix} \tag{A.4}$$

where A is the cross-sectional area, L is the length, E is the modulus of elasticity, I_z and I_y are the principal moment of inertia, and J is the torsional constant of a frame.

$$[K_g]_b = \frac{P}{L}\begin{bmatrix} 0 & 0 & 0 & 0 & 0 & 0 & 0 & 0 & 0 & 0 & 0 & 0 \\ & \frac{6}{5} & 0 & 0 & 0 & \frac{L}{10} & 0 & -\frac{6}{5} & 0 & 0 & 0 & \frac{L}{10} \\ & & \frac{6}{5} & 0 & -\frac{L}{10} & 0 & 0 & 0 & -\frac{6}{5} & 0 & -\frac{L}{10} & 0 \\ & & & 0 & 0 & 0 & 0 & 0 & 0 & 0 & 0 & 0 \\ & & & & \frac{2}{15}L^2 & 0 & 0 & 0 & \frac{L}{10} & 0 & -\frac{L^2}{30} & 0 \\ & & & & & \frac{2}{15}L^2 & 0 & -\frac{L}{10} & 0 & 0 & 0 & -\frac{L^2}{30} \\ & & & & & & 0 & 0 & 0 & 0 & 0 & 0 \\ & & & & & & & \frac{6}{5} & 0 & 0 & 0 & -\frac{L}{10} \\ & & & sym. & & & & & \frac{6}{5} & 0 & \frac{L}{10} & 0 \\ & & & & & & & & & 0 & 0 & 0 \\ & & & & & & & & & & \frac{2}{15}L^2 & 0 \\ & & & & & & & & & & & \frac{2}{15}L^2 \end{bmatrix} \tag{A.5}$$

where P is the axial force of a frame.

B. Element mass matrix

$$[M_e]_b = \rho AL\begin{bmatrix} \frac{1}{3} & 0 & 0 & 0 & 0 & 0 & \frac{1}{6} & 0 & 0 & 0 & 0 & 0 \\ & \frac{13}{35}+\frac{6I_z}{5AL^2} & 0 & \frac{11L}{210}+\frac{I_z}{10AL} & 0 & 0 & 0 & \frac{9}{70}-\frac{6I_z}{5AL^2} & 0 & 0 & 0 & -\frac{13L}{420}+\frac{I_z}{10AL} \\ & & \frac{13}{35}+\frac{6I_y}{5AL^2} & 0 & -\frac{11L}{210}-\frac{I_y}{10AL} & 0 & 0 & 0 & \frac{9}{70}-\frac{6I_y}{5AL^2} & 0 & \frac{13L}{420}-\frac{I_y}{10AL} & 0 \\ & & & \frac{I_x}{3A} & 0 & 0 & 0 & 0 & 0 & \frac{I_x}{6A} & 0 & 0 \\ & & & & \frac{L^2}{105}+\frac{2I_y}{15A} & 0 & 0 & 0 & -\frac{13L}{420}+\frac{I_y}{10AL} & 0 & -\frac{L^2}{140}-\frac{I_y}{30A} & 0 \\ & & & & & \frac{L^2}{105}+\frac{2I_z}{15A} & 0 & \frac{13L}{420}-\frac{I_z}{10AL} & 0 & 0 & 0 & -\frac{L^2}{140}-\frac{I_y}{30A} \\ & & & & & & \frac{1}{3} & 0 & 0 & 0 & 0 & 0 \\ & & & & & & & \frac{13}{35}+\frac{6I_z}{5AL^2} & 0 & 0 & 0 & -\frac{11L}{210}-\frac{I_z}{10AL} \\ & & & & & & & & \frac{13}{35}+\frac{6I_y}{5AL^2} & 0 & \frac{11L}{210}+\frac{I_y}{10AL} & 0 \\ & & sym. & & & & & & & \frac{I_x}{3A} & 0 & 0 \\ & & & & & & & & & & \frac{L^2}{105}+\frac{2I_y}{15A} & 0 \\ & & & & & & & & & & & \frac{L^2}{105}+\frac{2I_z}{15A} \end{bmatrix} \tag{B.1}$$

where I_x is the polar moment of inertia of a frame.

C. Conventional stability functions before modifications

In the case of tensile force P (P is positive),

$$\begin{aligned} S_{1z} &= \omega_z^3 \sinh\omega_z/(12R_t) \\ S_{2z} &= \omega_z^2(\cosh\omega_z - 1)/(6R_t) \\ S_{3z} &= \omega_z(\omega_z\cosh\omega_z - \sinh\omega_z)/(4R_t) \\ S_{4z} &= \omega_z(\sinh\omega_z - \omega_z)/(2R_t) \end{aligned} \tag{C.1}$$

$$R_t = 2 - 2\cosh\omega_z + \omega_z\sinh\omega_z \tag{C.2}$$

$$S_5 = 1/\{1 - EA(R_{tmy} + E_{tmz})/4P^3L^2\} \tag{C.3}$$

where

$$\begin{aligned} R_{tmy} &= \omega_y(M_{1y}^2 + M_{2y}^2)(\coth\omega_y + \omega_y\mathrm{cosech}^2\omega_y) \\ &- 2(M_{1y} + M_{2y})^2 + M_{1y}M_{2y}(1 + \omega_y\coth\omega_y)(2\omega_y\mathrm{cosech}\,\omega_y) \end{aligned} \tag{C.4}$$

$$\begin{aligned} R_{tmz} &= \omega_z(M_{1z}^2 + M_{2z}^2)(\coth\omega_z + \omega_z\mathrm{cosech}^2\omega_z) \\ &- 2(M_{1z} + M_{2z})^2 + M_{1z}M_{2z}(1 + \omega_z\coth\omega_z)(2\omega_z\mathrm{cosech}\,\omega_z) \end{aligned} \tag{C.5}$$

where

$$\omega_z = \mu_z L,\ \mu_z^2 = \frac{P}{EI_z},\ \omega_y = \mu_y L,\ \mu_y^2 = \frac{P}{EI_y} \tag{C.6}$$

In the case of compressive force P (P is negative),

$$\begin{aligned} S_{1z} &= \omega_z^3 \sin\omega_z/(12R_c) \\ S_{2z} &= \omega_z^2(1 - \cos\omega_z)/(6R_c) \\ S_{3z} &= \omega_z(\sin\omega_z - \omega_z\cos\omega_z)/(4R_c) \\ S_{4z} &= \omega_z(\omega_z - \sin\omega_z)/(2R_c) \end{aligned} \tag{C.7}$$

$$R_c = 2 - 2\cos\omega_z - \omega_z\sin\omega_z \tag{C.8}$$

$$S_5 = 1/\{1 - EA(R_{cmy} + R_{cmz})/4P^3L^2\} \tag{C.9}$$

where

$$\begin{aligned} R_{cmy} &= \omega_y(M_{1y}^2 + M_{2y}^2)(\cot\omega_y + \omega_y\mathrm{cosec}^2\omega_y) \\ &- 2(M_{1y} + M_{2y})^2 + M_{1y}M_{2y}(1 + \omega_y\cot\omega_y)(2\omega_y\mathrm{cosec}\,\omega_y) \end{aligned} \tag{C.10}$$

$$\begin{aligned} R_{cmz} &= \omega_z(M_{1z}^2 + M_{2z}^2)(\cot\omega_z + \omega_z\mathrm{cosec}^2\omega_z) \\ &- 2(M_{1z} + M_{2z})^2 + M_{1z}M_{2z}(1 + \omega_z\cot\omega_z)(2\omega_z\mathrm{cosec}\,\omega_z) \end{aligned} \tag{C.11}$$